Agglomeration defects on irradiated carbon nanotubes

Cássio Stein Moura, Naira Maria Balzaretti, Livio Amaral, Rodrigo Gribel Lacerda, and Marcos A. Pimenta

Citation: AIP Advances **2**, 012174 (2012); doi: 10.1063/1.3696884
View online: http://dx.doi.org/10.1063/1.3696884
View Table of Contents: http://aipadvances.aip.org/resource/1/AAIDBI/v2/i1
Published by the American Institute of Physics.

Agglomeration defects on irradiated carbon nanotubes

Cássio Stein Moura,[1] Naira Maria Balzaretti,[2] Livio Amaral,[2] Rodrigo Gribel Lacerda,[3] and Marcos A. Pimenta[3]

[1]*Faculty of Physics, Pontifícia Universidade Católica do Rio Grande do Sul, 90619-900, Porto Alegre, RS, Brazil*

[2]*Institute of Physics, Universidade Federal do Rio Grande do Sul, C.P.: 15051, 91501-070, Porto Alegre, RS, Brazil*

[3]*Universidade Federal de Minas Gerais, C.P.: 702, 31270-901, Belo Horizonte, MG, Brazil*

(Received 20 July 2011; accepted 16 February 2012; published online 13 March 2012)

Aligned carbon nanotubes (CNT) were irradiated in the longitudinal and perpendicular directions, with low energy carbon and helium ions in order to observe the formation of defects in the atomic structure. Analysis through Raman spectroscopy and scanning electron microscopy indicated bundle rupture and ion track formation on nanotube bundles. Aligned CNT presented a kind of defect comprising ravine formation and tube agglomeration on top of the substrate. The latter structure is possibly caused by static charge accumulation induced by the incoming ions. Fluence plays a role on the short range order. Higher fluence irradiation transforms CNT into amorphous carbon nanowires. [http://dx.doi.org/10.1063/1.3696884]

Several techniques can be used to modify carbon nanostructures aiming at the development of materials with peculiar physicochemical properties.[1] Ion irradiation creates collisional cascades that can lead to the production of defects inducing loss of crystallinity, polymerization, and junction creation, among others. In this work we investigated the effect of C^+ and He^+ irradiation on aligned and entangled bundles of carbon nanotubes (CNT). The samples were analyzed by Raman spectroscopy (RS) and scanning electron microscopy (SEM). Raman Line shift and intensity changes due to irradiation have been studied by other authors using various kinds of beams.

Ishaq *et al.*[3] used a 40 keV argon beam on multiwall carbon nanotubes (MWCNT) samples and observed junction formation within CNT. Moreover, amorphous carbon was formed and identified by the broadening of the *D* and *G* lines on the RS spectrum at room temperature. At a 800 K regime, the *D*-band became sharp indicating the maintenance of the crystal structure. Temperature increases atomic mobility which improves defects healing. At the high energy of 60 MeV and the low fluence of 1 x 10^{13} cm^{-2}, Kumar *et al.*[2] irradiated MWCNT with a Ni beam and observed a decrease on the Raman bands intensities. Such a regime causes a high level of damage on the system. Puech *et al.*[4] observed a down-shift on the Raman lines when electron irradiation at 2.5 MeV and 4.6 x 10^{18} cm^{-2} is performed on single-wall carbon nanotubes (SWCNT) and MWCNT. However, the lines intensities did not suffer alterations. Line shift was also observed by Hulman *et al.*[5] when SWCNT are irradiated by 1.3 MeV gamma-rays. The *D*-band position changes roughly 10 cm^{-1}. They also observed a *G*-band increase due to irradiation.

In this investigation CNT were produced in two different arrangements: aligned tubes perpendicular to the substrate surface and entangled tubes parallel to the surface. Details on the CNT growth is based on conditions reported previously.[6,7]

The as prepared samples were analyzed through SEM using a JEOL JSM 6060 microscope. A potential of 10 kV was employed in order to minimize sample damage while keeping good image quality. Figure 1 shows a typical image of the samples, revealing the good alignment among the tubes.

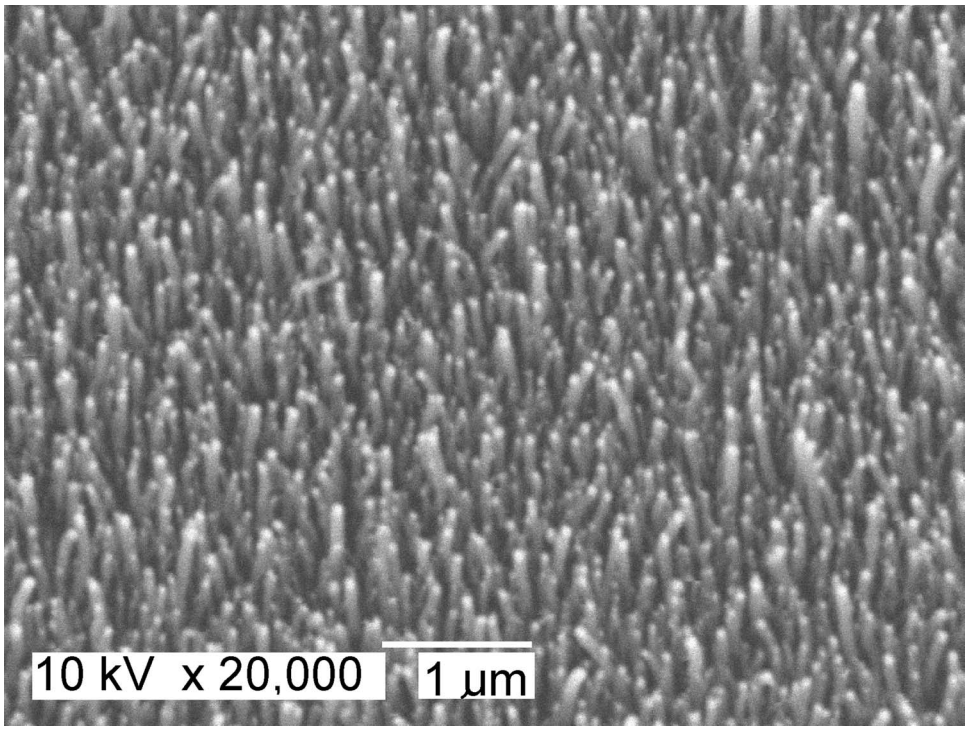

FIG. 1. SEM of as prepared CNT grown on top of a silicon substrate.

RS was performed on the samples as well. Figure 2(a) shows the Raman spectrum of the pristine aligned samples obtained using a 632.8 nm HeNe laser as the excitation source. The line at 523 cm^{-1} corresponds to the silicon substrate vibration mode. The line at 1320 cm^{-1} is related to the presence of impurities or defects in the graphene lattice. Its low intensity indicates the good quality of the samples. The lines at 1592 cm^{-1} and 2755 cm^{-1} correspond to the *G*- and the *G′*-band respectively.

Ion irradiation was performed on a Tandem accelerator with two kinds of projectiles. Low degradation was investigated using a 20 keV helium beam and high degradation was studied with a 50 keV carbon beam. Two values of beam fluences were used for each projectile: 1 x 10^{14} and 2 x 10^{15} cm^{-2}, which from now on will be referred as low and high fluences, respectively. All irradiations were performed along a direction perpendicular to the substrate surface. The SEM images revealed two different kinds of defects produced by ion irradiation on CNT bundles: single bundle rupture and ion track over long distances. Bundle rupture was observed for both types of projectiles and both fluences. Figure 3 shows the intermingled bundles after carbon irradiation at 2 x 10^{15} cm^{-2}. Most of the tubes are intact, but some of them are broken. The white dots on the picture show the breakage points were the bundles suffered a tip reconstruction process after the collision has taken place. Similar images were observed for helium atoms at both fluences.

The other type of defect shown by SEM, e. g., ion track, happened for both kinds of projectiles, except for helium at low fluence. Either such defect is not formed at low fluences or it is so rare that it was not possible to find it in the irradiated samples, even after an exhaustive scanning of the sample surface. Figure 4 shows a typical ion track formed on the bundles due to a C^+ irradiation at high fluence. A deep straight valley surrounded by a parallel ravine which smoothly goes from the bottom of the valley to the top level of the bundle layer is observed. Similar features were observed at low carbon fluence and high helium fluence. The SEM images of the aligned CNT irradiated at low fluence did not show any modification compared to the pristine sample images, being impossible to distinguish between them. However, when the aligned samples were irradiated by a high fluence beam, some strange structures were formed. Figure 5 shows an example of the structure formed on the aligned samples by high fluence He^+ irradiation. The white region seems to be a cluster of atoms that were drawn out of the surface and attached back on top of other tubes. At left one can observe

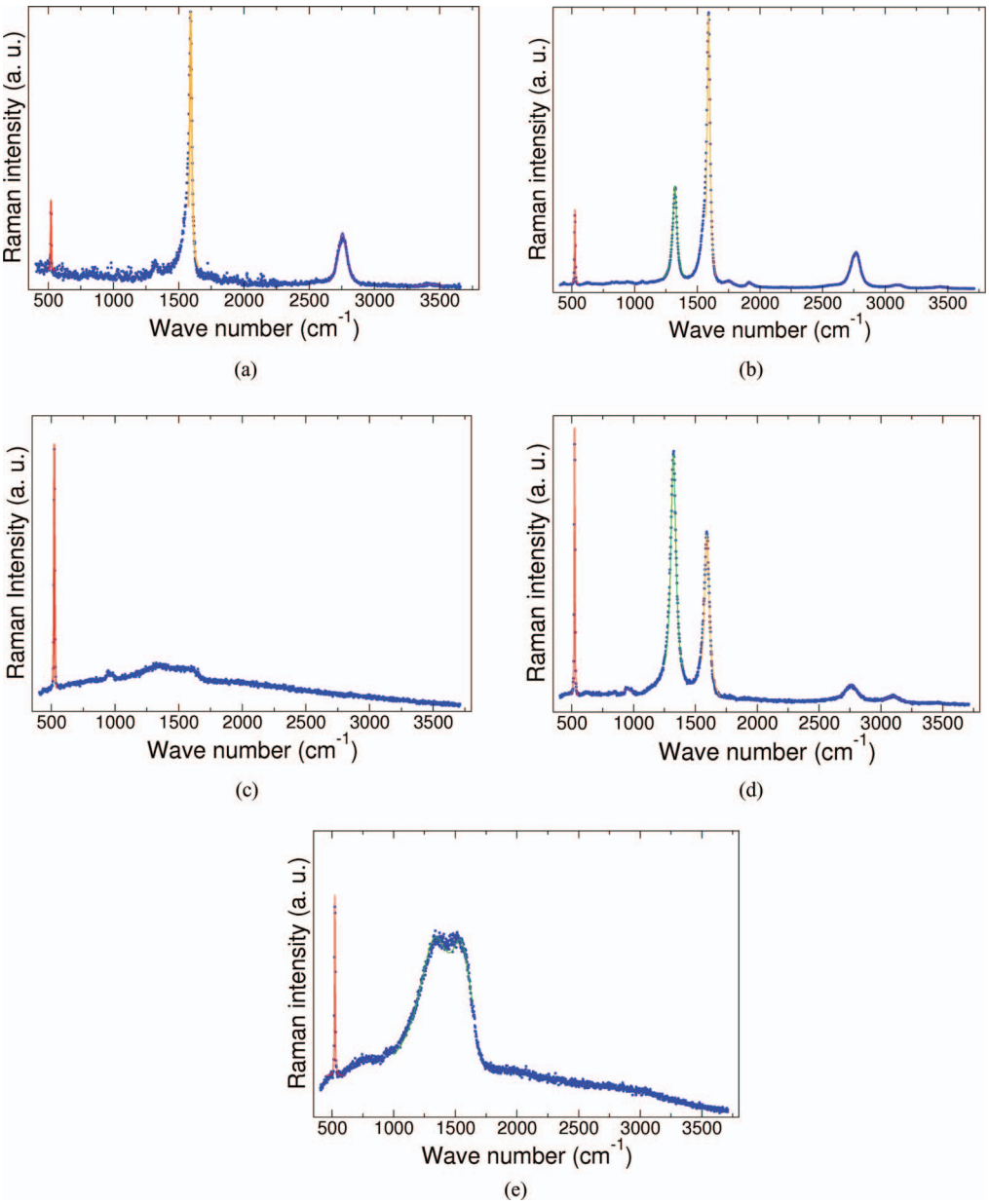

FIG. 2. Raman spectra of aligned CNT samples. Dots represent the experimental data and solid lines represent the numerical fitting. (a) As prepared samples. Irradiated samples: (b) 20 keV He^+, 1 x 10^{14} cm^{-2}; (c) 20 keV He^+, 2 x 10^{15} cm^{-2}; (d) 50 keV C^+, 1 x 10^{14} cm^{-2}; (e) 50 keV C^+, 2 x 10^{15} cm^{-2}.

several tubes that were tilted compared to the pristine remaining tubes which are seen on the right part of the picture. The feature shown in Fig. 5 was also present on the C^+ irradiated samples at a more frequent rate. A typical example is shown in Figure 6. A circular clearing was created and the tubes that were once perpendicularly attached to the substrate piled up at the center of the clearing.

A possible reason for these features generation could be related to sample manipulation, despite the great care used during handling the samples. In order to check such hypothesis some non-irradiated samples were deliberately scratched either with tweezers or rubbing one sample onto another. Figure 7 shows an image of such samples. One can notice that, differently from Figure 4, where a smooth transition between the valley and the sample surface could be seen, a steep transition is observed as if the tubes had been pulled out of the substrate surface. At the bottom of the valley

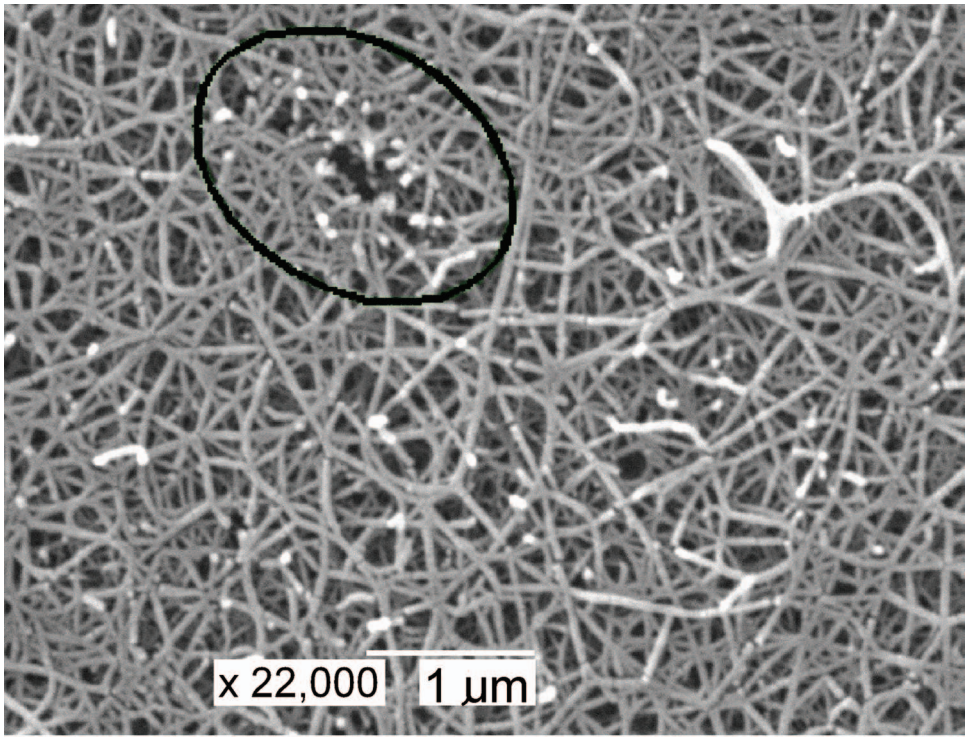

FIG. 3. SEM of CNT bundles irradiated with C^+ at 50 keV and 2 x 10^{15} cm^{-2}. Bundles ruptures happened in the region within the ellipse.

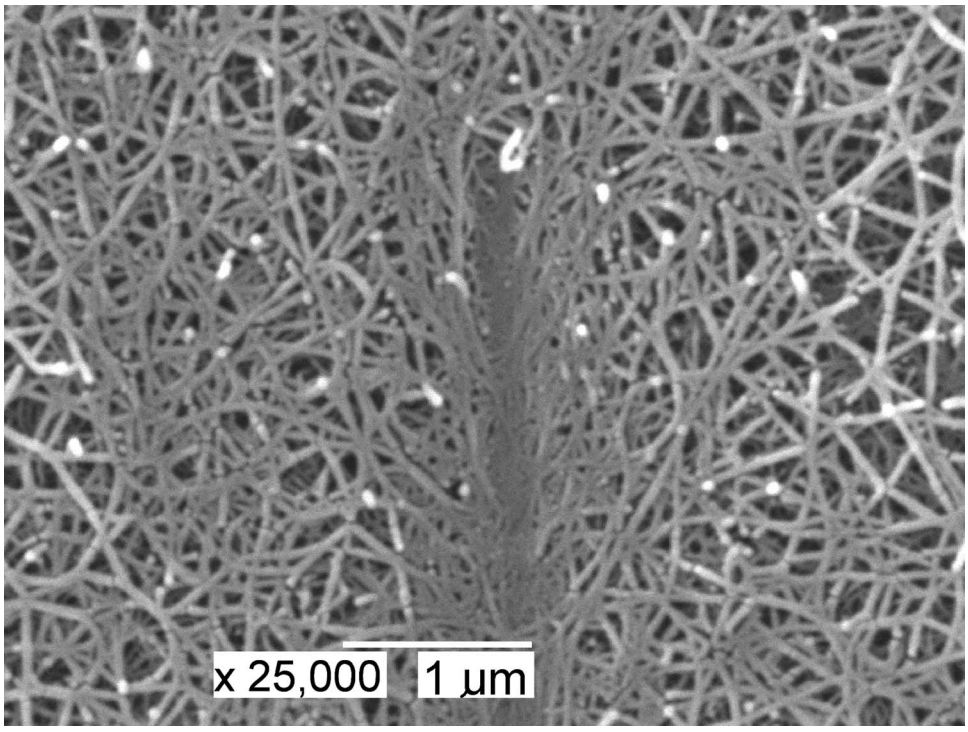

FIG. 4. Ion track formed on the entangled CNT bundles irradiated by C^+ at 50 keV and 2 x 10^{15} cm^{-2}. Bundle breakage can also be seen at the white dots.

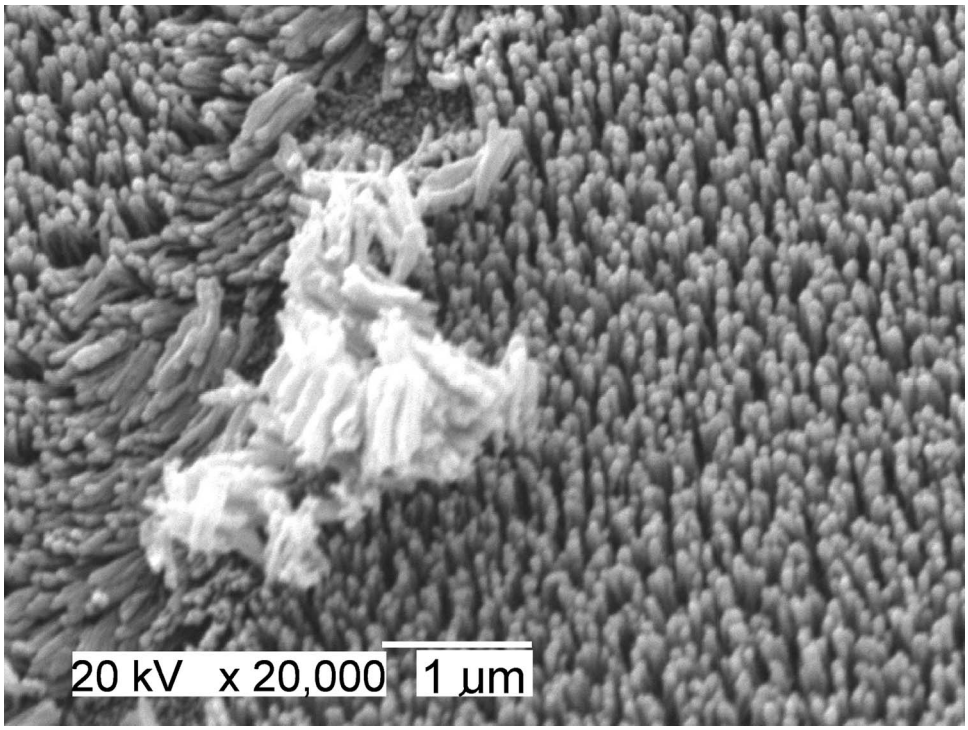

FIG. 5. Feature formed by He^{+} irradiation at 20 keV and 2 x 10^{15} cm^{-2} on tubes aligned perpendicular to the surface.

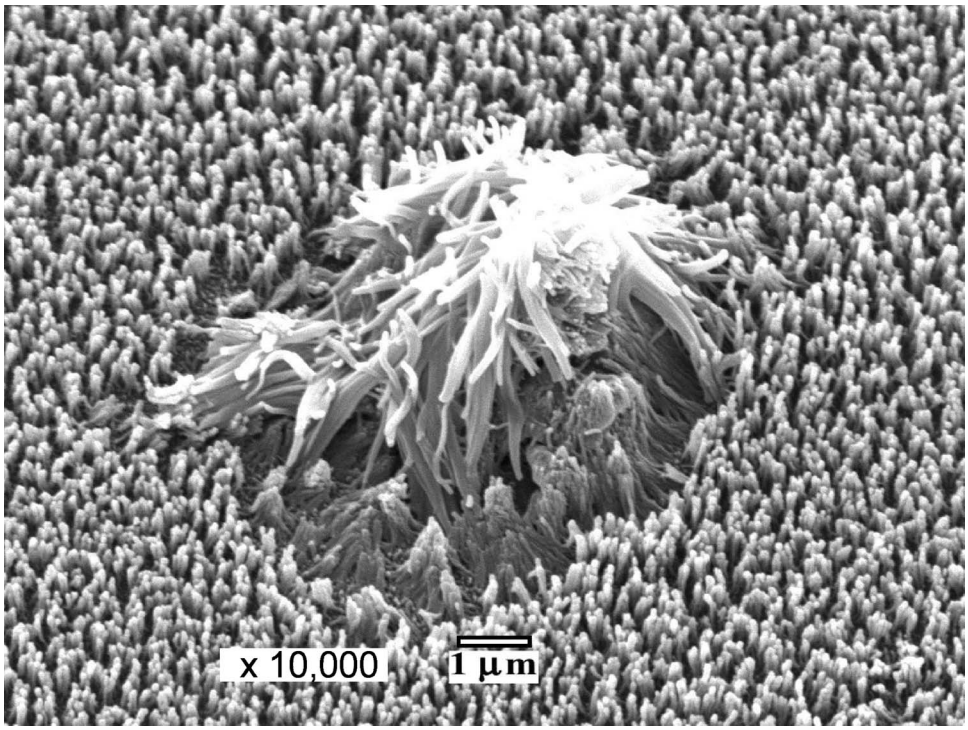

FIG. 6. Feature formed by C^{+} irradiation at 50 keV and 2 x 10^{15} cm^{-2} on tubes aligned perpendicular to the surface.

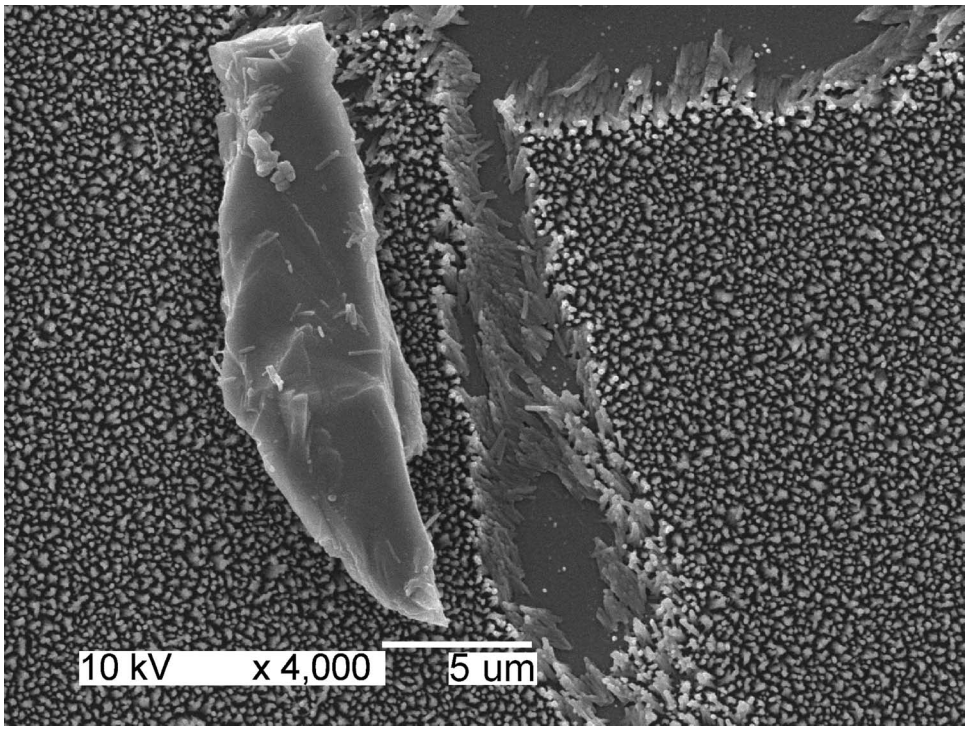

FIG. 7. SEM of an unirradiated sample deliberately scratched on the surface.

the plane substrate surface is shown. To the left of the valley, a grain of dust, which was probably aggregated during the deliberate manipulation, rests on top of the CNT. The clear difference on the steepness of the valley border between the defects shown in Figures 4 and 7 indicates that probably the feature observed in Figure 4 was not due to sample manipulation.

RS of the aligned samples was performed prior and after irradiation. In Figure 2(a) the Raman spectrum of a pristine sample is shown in which one can see the vibrational modes corresponding to well aligned tubes. The spectra of the irradiated samples are presented and discussed below.

Figure 2(b) shows the spectrum of an aligned CNT sample after irradiation with He^+ at 20 keV and 1 x 10^{14} cm^{-2}. Comparing to Figure 2(a), it is easy to see the main difference between both spectra which is the intensity increase of the line *D*-band at 1320 cm^{-1}, related to the presence of defects. Moreover, two lines seem to appear more clearly at 1752 and 1916 cm^{-1}. On the other hand, for the higher fluence of 2 x 10^{15} cm^{-2} at the same energy (Figure 2(c)), the spectrum indicates a loss of the nanotubes vibration mode indicating sample amorphization.

Figures 2(d) and 2(e) show the Raman spectra for the samples after irradiation with carbon ions at the low and high fluences, respectively. The effect of the low fluence irradiation is more pronounced when the C^+ beam hits the sample for the intensity of the *D*-band increased significantly compared to the sample irradiated with a He^+ beam at low fluence.

The SEM images show features on the CNT structure caused by irradiation, namely, a glancing path over the surface and a sort of agglomeration of CNT one on top of the others. We believe that those kinds of features were created by projectiles which reach the surface of the bundled CNT and gradually deliver their energy over the collisional path. When the beam is composed of the same atomic species as the target, e. g. carbon, the energy transfer is optimized, improving the possibility of creation of defects. This is why we observed such tracks even for the low fluence carbon beam. In the case of helium projectiles this sort of feature may happen although only for high fluence, since the light projectile is less efficient in creating defects on a carbon structure.

When the aligned CNT are hit by the high fluence beam a curious feature shows up, as seen on Figures 5 and 6. A possible physical explanation for the creation of such structures could be related to charge accumulation. The incoming ions accumulate electrical charge at a certain surface spot

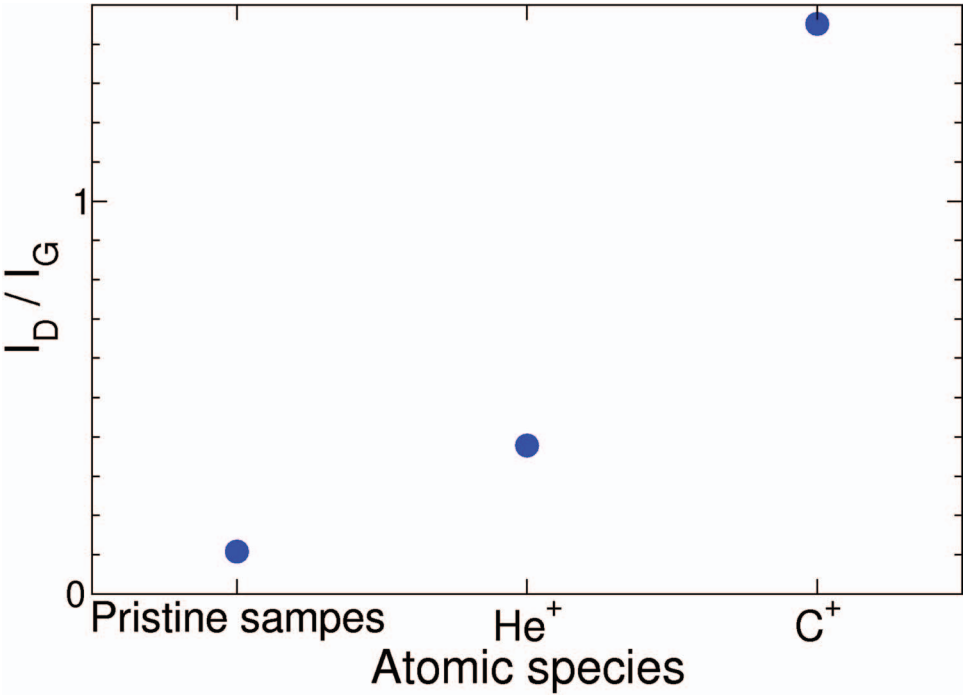

FIG. 8. Ratio of the *D* and *G* bands areas under the low fluence regime irradiation for both He^+ and C^+ compared to the pristine samples.

which is not able to spread out fast enough to be drained at ground. After charge reaches a certain threshold the coulombic repulsion between the tubes is high enough to produce a local explosion. The debris, after losing their charge, return to the sample surface and become piled up.

RS can describe sub-micrometric features. The spectrum of the pristine samples shown on Figure 2(a) reflects the great ordering of the nanotube forest grown on top of the substrate. A measurement of that order is the line intensities ratio I_D/I_G (Figure 8). When irradiation occurs, the ordering degree decreases, as shown by the increase on the I_D/I_G ratio. Figures 2(b) and 2(d) show the increase of the *D*-band peak relative to the *G*-band in both cases. Nonetheless, the disordering is larger for the carbon beam. We believe this fact is due to the improved energy transfer between the carbon projectiles and the carbon targets on the tubes. When the samples are irradiated by a high fluence beam the disordering is so intense that peaks on the Raman spectra spread out and convolute into a single broad line. Figures 2(c) and 2(e) show that the only unaffected peak is the one due to the silicon substrate at 523 cm^{-1}. The longitudinal structures perpendicular to the surface remain present even after the high fluence irradiation. We believe that besides the micrometric rearrangement shown by SEM, another type of restructuring occurs at nanoscale. The atoms sitting on the sites of the honeycomb lattice may be displaced ending up at places near the nanotube wall keeping the cylindrical form but with a decrease on the hexagonal ordering. Such rearrangement can be produced by as low energy as a couple hundred electron-volts as shown by molecular dynamics calculations.[8] Therefore, the nanotubes may be transformed into amorphous nanowires under irradiation.

We may conclude that aligned CNT are damaged in different ways at the micro- and nanoscale. SEM shows a kind of rearrangement similar to a micrometric nanotube mountain drawn off of the substrate surface due to static electricity accumulated owing to the incoming ions. The Raman spectra of the low fluence irradiated sample show the presence of a narrow and strong *D*-band, reflecting the creation of local defects in the honeycomb nanotube structure. The density of local defects was observed to be higher when the sample was irradiated with carbon atoms. In the case of the high fluence irradiated samples, the Raman spectra exhibited only broad bands, which are typical of amorphous carbon. Nonetheless, the tubes kept their longitudinal shapes, but their internal

structure was altered. Amorphous carbon nanowires can be produced by high fluence irradiation of CNT.

The authors acknowledge the Brazilian funding agencies CNPq and CAPES for their financial support.

[1] C. S. Moura, *New carbon materials, basic science and applications*, (Edipucrs, Porto Alegre, 2009).
[2] A. Kumar, F. Singh, P. M. Koinkar, D. K. Avasthi, J. C. Pivin, M. A. More, Thin Solid Films **517**, 4322-24 (2009).
[3] A. Ishaq, Z. Nia, L. Yana, J. Gonga, D. Zhua, Rad. Phys. Chem. **79**, 687-91 (2010).
[4] P. Puech, E. Flahaut, A. Bassil, T. Juffmann, F. Beuneu, W. S. Bacsa, J. Raman Spect. **38**(6), 714-20 (2007).
[5] M. Hulman, V. Skákalová, S. Roth, H. Kuzmany, J. Appl. Phys. **98**, 024311-5 (2005).
[6] M. S. Bell, R. G. Lacerda, K. B. K. Teo, N. L. Rupesinghe, G. A. J. Amaratunga, W. I. Milne, M. Chhowalla, Appl. Phys. Let. **85**(7), 1137-9 (2004).
[7] R. G. Lacerda, A. S. The, M. H. Yang, K. B. K. Teo, N. L. Rupesinghe, S. H. Dalal, K. K. K. Koziol, D. Roy, G. A. J. Amaratunga, W. I. Milne, M. Chhowalla, D. G. Hasko, F. Wyczisk, P. Legagneux, Appl. Phys. Let. **84**(2), 269-71 (2004).
[8] C. S. Moura, L. Amaral, Carbon **45**(9), 1802-7 (2007).